



Effects of Spatial Variability, Associated with a Frontal Structure, on Predictions of Age-0 Walleye Pollock (*Theragra chalcogramma*) Growth around the Pribilof Islands, Bering Sea

L. Ciannelli*

School of Aquatic and Fishery Sciences, University of Washington, Seattle, U.S.A.

Received 1 February 2001 and accepted in revised form 16 August 2001

Age-0 walleye pollock growth along a frontal transect around the Pribilof Islands, Bering Sea, was estimated by using a spatially-explicit bioenergetics model. Predicted growth patterns along the transect were tested against the spatial resolution of the model, to examine the extent to which informative results were affected by the input spatial resolution. Results of model implementation to the Pribilof Islands scenario showed that on average fish residing in the offshore region of the transect were exposed to areas in which growth potential was two to three times higher than in the inshore region. Modelling results corroborated well with independent indicators of age-0 pollock growth, such as age-specific length and Fulton condition index from fish collected at the same location examined with the model. In spite of the better feeding and growth potential of the offshore region, age-0 pollock were found mainly in the inshore portion of the transect. Evidently, other factors, besides habitat energetics, needed to be considered to explain the distribution of age-0 pollock around the islands. Predictions of age-0 pollock growth along the transect were highly sensitive to the input spatial resolution of the model, but only at a spatial scale larger than a threshold of about 1000–2500 m. It is proposed that such threshold represents the limit beyond which important physical and biological boundaries are crossed and consequently model predictions derived from average conditions become biased.

© 2002 Elsevier Science Ltd. All rights reserved.

Keywords: age-0 pollock; *Theragra chalcogramma*; spatial-explicit models; bioenergetics; fronts; Pribilof Islands; Bering Sea

Introduction

In the southeastern Bering Sea, the Pribilof Islands are an important nursery ground for age-0 pollock, *Theragra chalcogramma* (Pallas), and have been defined as a center of abundance of juvenile pollock in the east Bering Sea (Traynor & Smith, 1996). Many juvenile pollock predators, such as groundfish (Lang *et al.*, 2000), seabirds (Decker & Hunt, 1996) and marine mammals (Sinclair *et al.*, 1993), and pollock prey, such as euphausiids and copepods (Brodeur *et al.*, in press; Flint *et al.*, in press), are also present at high densities around the islands. Thus, the Pribilof Archipelago represent a pivotal location to study ecological interactions between age-0 pollock and their predators and prey in the Bering Sea.

Physical features of the water adjacent to the Pribilof Islands may play an important role in creating and concentrating such a rich and diverse community. Except for the Aleutian Islands, the Pribilof

Archipelago is the only emerged landmass in the vicinity of the Bering Sea slope. During summer, tides and winds create a thermal frontal around each of the two major islands (Coyle & Cooney, 1993), St. Paul and St. George. The frontal system is composed of a frontal region, which divides a well-mixed inshore region from a typical two-layered thermally stratified offshore region (Stabeno *et al.*, 1999). The extension of each region varies from 2 km, up to 20 km, depending mainly on the intensity of water stratification and wind forcing (Stabeno *et al.*, 1999). Previous studies have shown that physical heterogeneity around the Pribilofs can affect the biological system as well, structuring a variety of different communities within each frontal region (Coyle & Cooney, 1993; Brodeur *et al.*, 1997; Flint *et al.*, in press).

Growing fast and avoiding predation are keys to high survival of fishes, especially for juvenile stages of species residing in cold and highly seasonal environments (Houde, 1987, 1989). It is possible that age-0 pollock residing around the Pribilof Islands experience high growth rates due the high density of prey and the

*Mailing address: NOAA NMFS RACE, 7600 Sand Point Way NE, Seattle WA 98115, U.S.A. E-mail: Lorenzo.Ciannelli@noaa.gov

thermal heterogeneity associated with frontal sub-habitats (Brandt, 1993). However, given the high density of predators also present around the islands, age-0 pollock might also experience high predation mortality (Sinclair *et al.*, 1993; Lang *et al.*, 2000). To date, the relative benefits of an enhanced growth rate versus the negative effects of high predation on age-0 pollock population ecology around the Pribilof Islands are not known. The answer to this question must start with a quantitative estimate of both growth and predation effects on age-0 pollock density and distribution. Furthermore, given the high physical and biological heterogeneity associated with the frontal structure around the islands, it is recommended to explicitly account for spatial variability (Mason & Brandt, 1996).

The objectives of this study were twofold. First, to build a spatially-explicit bioenergetics model representative of age-0 walleye pollock residing around the frontal structure of the Pribilof Islands. Second, to apply the model to the Pribilof Islands region with the goal of quantifying the effect of various physical and biological factors, associated with frontal sub-habitats, on juvenile pollock growth. Spatially-explicit bioenergetics models have been developed to quantify the impacts of environmental heterogeneity on fish population ecology over a multitude of diverse habitats and results have improved our understanding of habitat utilization (Brandt *et al.*, 1992; Brandt, 1993; Mason *et al.*, 1995; Gieske *et al.*, 1998). However, spatially-explicit modelling is a data demanding process, since the spatial array of the modelled environmental factors often needs to be known at a high resolution (Brandt *et al.*, 1992). Furthermore, because of the many assumptions inherent of bioenergetics modelling (Ney, 1993), it is important to validate model predictions with independent measures of fish growth (Boisclair, 2001). Thus, in the final part of this study, I tested the effect of progressively lower spatial resolution on the model predictions of age-0 growth potential along the frontal transect, with the goal of examining the extent to which informative results were affected by the input spatial resolution of the model. Also, I validated age-0 pollock predicted growth along the frontal transect with two other indices of age-0's growth, independently collected along the same transect and time of the year inspected with the spatially-explicit bioenergetics model.

Materials and methods

Model description

The general model used to calculate fish growth is based on the Winberg (1956) balanced energetics

equation, in which, for a non-reproductive fish, all energy ingested (I) is allocated between metabolism (M), egestion (F), excretion (U) and growth (G):

$$G = I - M - F - U \quad (1)$$

Equation 1 is composed by two sub-models, a foraging model to calculate fish consumption (I) given prey density, water column temperature and predator size (Gerristen & Strickler, 1976), and a bioenergetics model to calculate fish growth (G), given foraging consumption, water temperature and physiology (Hewett & Johnson, 1992). All model equations are listed in Table 1. The foraging and bioenergetics portion of the model parameterized for age-0 pollock were validated against published values, derived either from field or laboratory evaluations.

Following the Brandt *et al.* (1992) approach, the forage plus bioenergetics model was made spatially-explicit by applying it to many different portions of the environment. Such portions of the environment, cells, differ from each other by specific physical and biological variables, including temperature, prey density, fish length and diet composition. The resulting output of the model, fish growth potential, indicates the potential growth of a fish if it were to inhabit that particular portion of the environment. In this study, the model was used to estimate age-0 pollock growth only within their distribution predicted from hydroacoustic analysis (Swartzman *et al.*, 1999a, b).

The spatial resolution of the model used in this study was 42 m in horizontal length and 1 m in depth. In general, the dimension of a cell depends mainly on the environmental heterogeneity and on the resolution of the sampling gear (Brandt & Mason, 1994; Mason & Brandt, 1996). The sampling resolution of this study was rather high because of the use of multi-frequency hydroacoustics to estimate fish and prey density in the water column (see below). Therefore the dimension of the cell was matched to the dimension of the smallest observed fish or zooplankton patch. Since the sampled transect along the whole frontal region was 50 000 m long at an average depth of 50 m, the full data matrix had about 60 000 elements.

Model parameterization

A summary of the model parameter values and units is shown in Table 2. Most of the bioenergetics model are described in Ciannelli *et al.* (1998). The newly introduced modelling portions were the foraging model (Equation 2), the predator swimming speed model

TABLE 1. Equations of forage and bioenergetics model used to estimate age-0 pollock growth potential. F_t =feeding time (min), T =water temperature ($^{\circ}\text{C}$), W_t =weight (g), N =food density (g m^{-3}). For description of other parameters see Table 2

Growth ($\text{g g}^{-1} \text{d}^{-1}$)	$G=I-M-F-U$	1
Ingestion ($\text{g g}^{-1} \text{d}^{-1}$)	$I=\text{Min}\left(\frac{I_f}{W_t}, I_{\text{max}}\right)$	—
Forage ingestion (g d^{-1})	$I_f=P\frac{\pi r^2 N}{3}\frac{3v^2+u}{v}F_t$	2
Maximum ingestion [§] ($\text{g g}^{-1} \text{d}^{-1}$)	$I_{\text{max}}=C_a W^{C_b} F(T)$	—
Predator swimming speed (cm s^{-1})	$vel \uparrow = A_{ct} W^{*k} e^{\beta T}$ if $T < r_{tl}$, $vel = R_{k1} W^{*k}$ if $T > r_{tl}$	3
Metabolism ($\text{g O}_2 \text{g}^{-1} \text{d}^{-1}$)	$M = a_r W^{B_r} e^{Q_r T} e^{A_c vel} + SDA$	4
Egestion	$F = I F_a$	—
Excretion	$U = I U_a$	—
Specific dynamic action	$SDA = (I - F) * D_s$	—

[§]For parameters of I_{max} see Ciannelli *et al.*, 1998.

[¶]Note: $1 \text{ cm s}^{-1} = 3/5 \text{ m min}^{-1}$, and forage swimming speed (v) is 1.5 times higher than the cruising speed (vel), therefore $v = 1.5 * 3/5 vel$.

TABLE 2. Descriptions and values of the parameters used in the spatially-explicit bioenergetics model of age-0 walleye pollock growth

Symbol	Description	Value and Units	Source
I	Consumption	(g g⁻¹ day⁻¹)	
P	Capture probability	0.35	1, 2, 3
v	Predator foraging swimming speed	0.1 m	see <i>vel</i>
u	Prey swimming speed	0.12 m min ⁻¹	4
r	Predator reactive distance	0.1 m	1, 5, 6, 7, 8
vel	Predator cruising swimming speed	(cm s⁻¹)	
A_{ct}	Intercept at $T=0^{\circ}\text{C}$	2.86	9, 10
R_{k1}	Intercept at $T=r_{tl}$	5.21	9, 10
β	Slope parameter	0.32	this study
K	Slope parameter	0.06	9, 10
r_{tl}	Temperature threshold	10 $^{\circ}\text{C}$	this study
R	Respiration	(g O₂ g⁻¹ day⁻¹)	
a_r	Intercept parameter	0.0034	11
B_r	Slope parameter	-0.251	11
Q_r	Temperature dependence coefficient	0.058	11
A_c	Slope parameter	0.1	this study
SDA	Specific Dynamic Action	—	11
F	Egestion		
F_a	Proportion of egested consumption	0.15	11
U	Excretion		
U_a	Proportion of excreted consumption	0.11	11

1. Utne-Palm (1999); 2. Viitasalo *et al.* (1998); 3. McLaughlin *et al.* (2000); 4. Yamazaki and Squires (1996); 5. Utne (1997); 6. Breck and Gitter (1982); 7. Flore *et al.* (2000); 8. Sweka and Hartman (2001); 9. Ryer and Olla (1997); 10. Ryer and Olla (1998); 11. Ciannelli *et al.* (1998).

(Equation 3) and the active metabolic rate defining the increase in respiration rate due to swimming and temperature (Equations 3 and 4). For some newly modelled processes there were no available laboratory

data to support the choice of parameters values. In such cases I used values either derived from phylogenetically and ecologically similar species, or simply values that would produce reasonable output.

Age-0 pollock reactive distance (r) to prey was set at 10 cm (0.1 m). To date, there are no studies done on walleye pollock reactive distance; therefore, I used a value approximated from studies done in other saltwater and freshwater species. With respect to saltwater species, Utne (1997) and Utne-Palm (1999) found that 40 to 45 mm gobies (*Gobiusculus flavescens*) feeding on large transparent copepods had a reactive distance ranging from about 8 to 12 cm depending mainly on water turbidity. With respect to freshwater species, Breck and Gitter (1982) found that 43 mm bluegill (*Lepomis macrochirus*) exposed to various sizes of *Daphnia* had a reactive distance ranging from 12 to 35 cm. However, their experiments were conducted in clear water and saturating light intensity ($7.5\text{--}8.5 \mu E s^{-1} m^{-2}$), therefore overestimating reactive distances in field conditions. Flore *et al.* (2000) found that 0+ nase (*Chondrostoma nasus*) had reactive distances ranging from about 11 to 20 cm depending on speed of water flow in the experimental unit and on the size of the fish (20–45 mm). Finally, Sweka and Hartman (2001) found that adult brook trout (*Salvelinus fontinalis*) (average length 136 mm) feeding on housefly larvae had reactive distances ranging from 12 to 80 cm, depending mainly on water turbidity.

Predator capture and ingestion probability (P) upon prey encounter, was set to 0.35, also based on experimental studies conducted in other saltwater and freshwater species. Utne-Palm (1999) found that 40–45 mm gobies feeding on copepods had a probability of attack upon detection of 0.27. Viitasalo *et al.* (1998) found that 15–18 mm stickleback (*Gasterosteus aculeatus*) feeding on calanoid copepods had a capture probability upon prey detection of 0.53. However neither studies estimated the probability of ingestion upon capture. Finally, McLaughlin *et al.* (2000) estimated that newly emerged brook trout (*Salvelinus fontinalis*) ate on average 42% of the detected prey in field conditions.

The intercept (A_{ct}) and slope (k) of the function relating age-0 pollock non-feeding swimming speed (vel) versus body size were derived from Ryer and Olla's (1997, 1998) experimental studies. The value obtained for the slope parameter (k) was equal to 0.32, the value obtained for the intercept (A_{ct}) was equal to 5.21 cm s^{-1} at an average experimental temperature of 10°C . This value was adjusted to 0°C assuming an exponential relationship between water temperature and fish swimming speed with slope parameter, β , equal to 0.06 (Equation 3). The temperature adjusted intercept value was then 2.86 cm s^{-1} . The value of β was chosen arbitrarily, due to lack of experimental studies relating age-0 pollock swimming speed to water temperature.

However this value was intentionally set similar to Q_r , the analog slope parameter relating respiration rate to water temperature, for which there were more experimental data available. In setting β similar to Q_r , it was assumed that swimming speed and metabolic expenditures increased at similar rates with increasing temperature. Temperature beyond which fish swimming speed becomes a function of fish body size only, rtl , was set equal to 10°C . Two hours of active foraging time (F_f) for fish feeding on zooplankton were allowed in the model, based on the gut evacuation curve shown in Brodeur *et al.* (2000). Predator foraging swimming speed, v , was that derived from the swimming speed sub-model (Equation 3, for parameter values see above) and multiplied by 1.5 to allow an increase in speed during foraging time (Ryer & Olla, 1997, 1998). Prey swimming speed of the foraging model, u , was set to 0.12 m min^{-1} (0.2 cm s^{-1}), after Yamazaki and Squires (1996) study on copepods.

The slope (B_r), intercept (a_r), and exponential slope (Q_r) relating age-0 pollock respiration to fish body size and environmental temperature (Equation 4) were derived from Ciannelli *et al.* (1998) and adapted to the different sub-model type used in this study. The slope of the equation relating fish swimming speed to active metabolic multiplier, A_{cs} , was set to 0.1, in order to fit values of the activity multiplier included in the range proposed by Ware (1975) for planktivorous fish.

Model implementations, assumptions and validation

The spatially-explicit bioenergetics model was applied to an existing data set collected along Line A, north of the Pribilof Islands (Figure 1), during September 1995. Field data required to run the model include prey density, water column temperature, age-0 pollock size distribution and age-0 pollock diet. Juvenile pollock prey density was estimated with acoustic sampling along Line A. Acoustic data were collected using SIMRAD EK500 at three different frequencies: 38, 120 and 200 KHz. Signal processing analysis allowed discrimination between zooplankton and fish, based mainly on differences in backscatter properties between the two classes of organisms at the three frequencies used. There were five acoustic passes during 1995, two during night hours, two during day hours and one at twilight. For a detailed description of the acoustic analysis and data corroboration see Swartzman *et al.* (1999a; b).

Temperature data were obtained from CTD casts done along Line A prior to the acoustic sampling. Casts were made in the shortest time possible to minimize the confounding effect of tidal currents on water column hydrography, and were spaced about

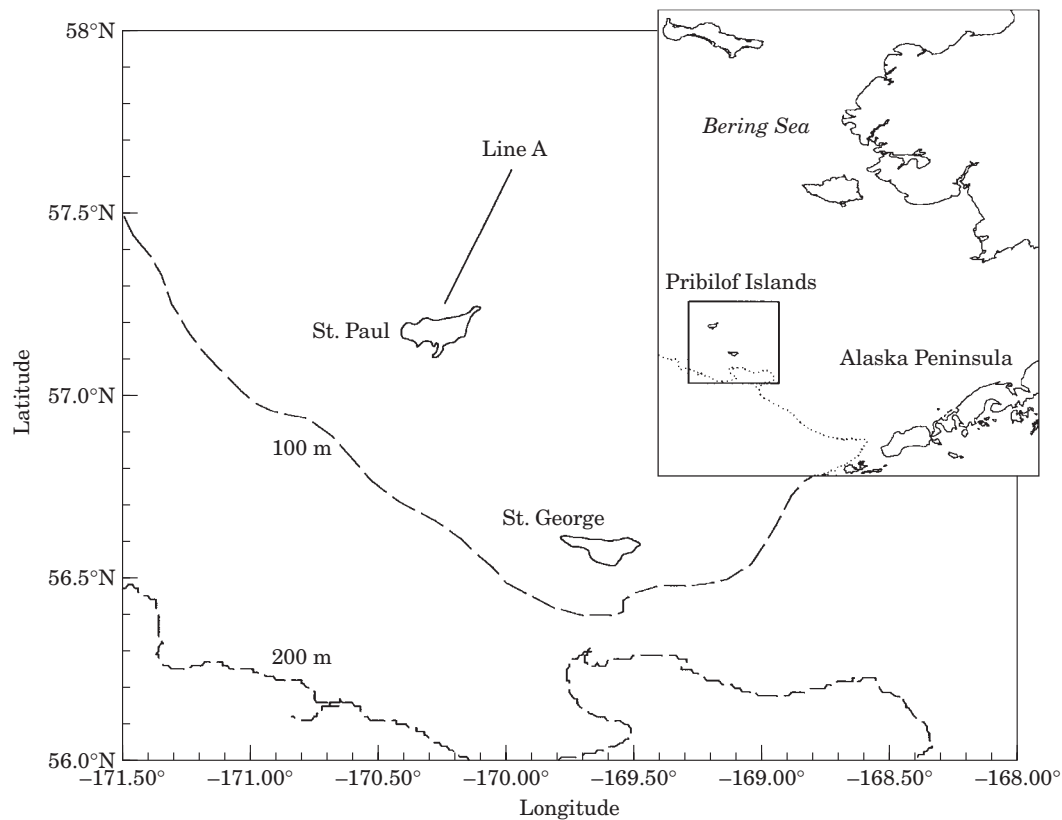


FIGURE 1. Study area and location of transect (Line A) where sampling took place during September 1995.

5–10 km from each other. Total distance from shore to the end of Line A was about 50 km. For a detailed description of the physical environment around the Pribilof Islands see [Stabeno *et al.* \(1999\)](#).

Age-0 pollock size distribution and diet were estimated from fish collected in midwater trawls contemporary to the acoustic sampling along Line A ([Brodeur *et al.*, 1997, 2000](#)). Midwater sampling took place over three hydrographic habitats, inshore, front and offshore. In 1995, four midwater tows were made at the inshore and offshore habitats, and six at the front habitat. According to [Stabeno *et al.* \(1999\)](#), the boundaries among the hydrographic habitats were chosen based on vertical temperature profile. The boundary between the inshore and front region corresponded to the first weakly stratified temperature profile. The boundary between the front and offshore region corresponded to the location where the temperature profile showed a two-fold decrease between the surface and subsurface levels of the thermocline. Within a particular habitat type, fish size assigned to each modelling cell was based on the size distribution derived from the analysis of midwater samples.

Similarly, in each cell within each habitat, fish diet, or for modelling purpose, caloric content of fish diet, was a weighted average of caloric density of prey present in the stomachs of fish collected within the considered habitat. Caloric content of prey items was taken from [Davis *et al.* \(1998\)](#).

Because of the hydroacoustic derivation, zooplankton density was in backscatter units rather than biomass units. To transform backscatter units to biomass units an arbitrary zooplankton calibration factor (z) was adopted. From the foraging model ([Equation 2](#)), if food is below saturation, there is a linear dependence between food density and fish consumption and growth. Consequently fish growth, derived from backscatter, is biased by a constant and ‘unknown’ amount. Because the objective of this analysis was to compare growth potential from different areas along the sampled transect, using prey backscatter as a proxy for prey biomass, should not affect the qualitative conclusions drawn (but see discussion).

Fish growth potential was calculated over an average zooplankton distribution transect. The average distribution transect was obtained by setting

zooplankton density below each horizontal bin (42 m), equal to the average zooplankton density throughout the depth of that particular horizontal bin and among the five passes performed along the transect. Thus, in the average distribution transect, zooplankton density does not change with depth, but rather with distance from shore. However, fish growth potential does change with depth, due to temperature differences throughout the water column. The assumption, in deriving the average distribution transect, was that even if zooplankters were vertically distant from a particular fish school, they would eventually move towards the school, due to the diel vertical migration of zooplankton.

Model predictions of age-0 pollock growth along Line A were validated against two independent growth indices, age-specific length and Fulton condition index ($\text{Weight (g)}/\text{StandardLength}^3 (\text{mm}) \times 10^5$). Fish used in the analysis of growth indices were collected during the same time of the year investigated in this study, over the inshore, front and offshore of Line A (Brodeur *et al.*, in press). Statistical differences between mean age-specific length among habitats were investigated with an ANCOVA (standard length covariate), while differences in Fulton index were investigated with an ANOVA. In both cases, multiple comparisons among groups were performed with a Tukey test.

Spatial resolution analysis

The effects of progressively lower spatial resolution, i.e. higher cell sizes, was tested on the estimated spatial distribution of age-0 pollock growth potential along Line A (spatial pattern). There were four pieces of data entered in a spatially-explicit fashion, namely, prey density, water column temperature, age-0 pollock size and age-0 pollock diet. Of these four, only the first three were varied in the spatial resolution analysis, because caloric content of fish diet changed little along the transect (see results). The effect of a particular spatial resolution on the spatial pattern of age-0 pollock growth potential was quantified by measuring the sum of the absolute residuals (SAR) between the maximum implemented resolution and the currently investigated resolution:

$$SAR = \sum_1^Q |MGP_i - CGP_i|$$

where Q =total number of fish schools along the transect, MGP =growth potential at maximum implemented resolution (cell size: 42 m \times 1 m),

CGP =growth potential at currently investigated spatial resolution.

Results

Environmental and biological variables

In September 1995, the temperature profile along Line A showed a strong vertical and horizontal differentiation (Figure 2). In the stratified offshore region average temperature of bottom and top layers were 3.1 °C and 9.5 °C, respectively, while average temperature in the inshore mixed region was 6.8 °C. The Bering Sea, during early 1995, had an extremely cold winter that extended its effects onto late summer, resulting in cold bottom temperatures and the observed strong habitat differentiation around the Pribilof Islands region. In other years, thermal differentiation among frontal regions of Line A was considerably less than that observed in 1995 (Stabeno *et al.*, 1999).

In 1995, density, size distribution, and diet of age-0 pollock along Line A changed according to the hydrographic habitat considered. Age-0 pollock density from midwater sampling was highest in the inshore (4.33 fish 100 m⁻³, SE=0.64) and front (3.97 fish 100 m⁻³, SE=0.97) habitats while it was lowest in the offshore (1.36 fish 100 m⁻³, SE=0.41) habitat. Moreover, inshore and frontal fish were larger than the offshore fish—average standard length of age-0 pollock was 53.4 mm in the inshore region, 53.1 mm in the frontal region and 48.9 mm in the offshore region (Brodeur *et al.*, 1997). Differences in age-0 pollock length were mainly due to earlier hatch date of inshore and front fish, rather than differences in growth rate (see age-specific length analysis). Age-0 pollock diet by weight was mainly composed of copepods in offshore habitat (54.8%), while in the inshore and frontal habitats, euphausiids (13.0% inshore and 22.8% front), in addition to copepods (45.3% inshore and 37.6% front), were well represented in the diet (Table 3).

Hydroacoustic estimates of zooplankton and age-0 pollock distribution along Line A confirmed the trend observed in the midwater samples: higher fish density was detected toward middle and inshore portion of the transect. In contrast, detected zooplankton density was highest toward the offshore region (Swartzman *et al.*, 1999b) (Figure 2). From the acoustic analysis it appeared that fish were residing mostly above the thermocline and diel vertical migration of fish was rarely observed. Unlike fish, zooplankton patches were actively migrating in the water column, coming

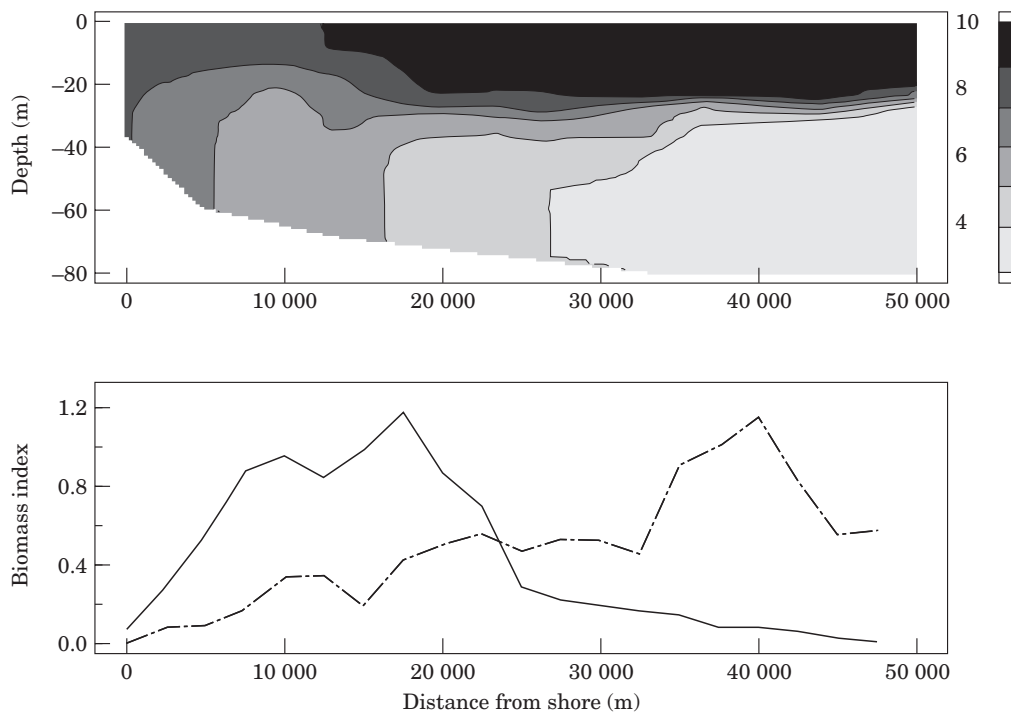


FIGURE 2. Upper panel: Temperature ($^{\circ}\text{C}$) profile along Line A, during September 1995. Lower panel: acoustically derived distribution of age-0 pollock (—) and zooplankton (---) along the same line and time of the year. In graph, solid line indicates the average value among five hydroacoustics passes and is calculated beneath a 2500 m running distance bin.

TABLE 3. Age-0 pollock diet (proportion of weight) and prey caloric content in three habitat types along Line A. Caloric content of prey items are from Davis *et al.* (1998)

	Inshore	Front	Offshore	Cal g wet wt ⁻¹
Chaetognaths	0.042	0.086	0.004	488
Crustacea	0.026	0.030	0.008	966
Euphausiids	0.130	0.228	0.021	743
Amphipods	0.007	0.000	0.022	589
Copepods	0.453	0.376	0.548	627
Larvacea	0.000	0.010	0.024	759
Fish	0.034	0.000	0.024	1374
Pteropod	0.026	0.096	0.157	624
Ostracod	0.010	0.000	0.017	743
Unident.	0.272	0.174	0.175	—
Weighted calories	688.4	658.1	658.6	

above the thermocline during the night and going down during the day (Swartzman *et al.*, 1999b).

Corroboration of forage and bioenergetics model

The sub-model portions that were first included in this study were tested against the range of environmental variables encountered in the field data, to verify that the model was indeed producing reasonable

results. Environmental variables that were explicitly accounted for were fish mass, zooplankton density and water column temperature. Fish mass ranged from 0.41 g to 8.04 g (median 0.97 g, mean 1.22 g). Calibrated zooplankton density ranged from 0 to 0.07 (median 0.024, mean 0.026). Temperature ranged from 2.7 to 9.7 $^{\circ}\text{C}$ (Figure 2).

Fish consumption, as predicted from the forage sub-model, ranged from 0 (in the absence of food) to

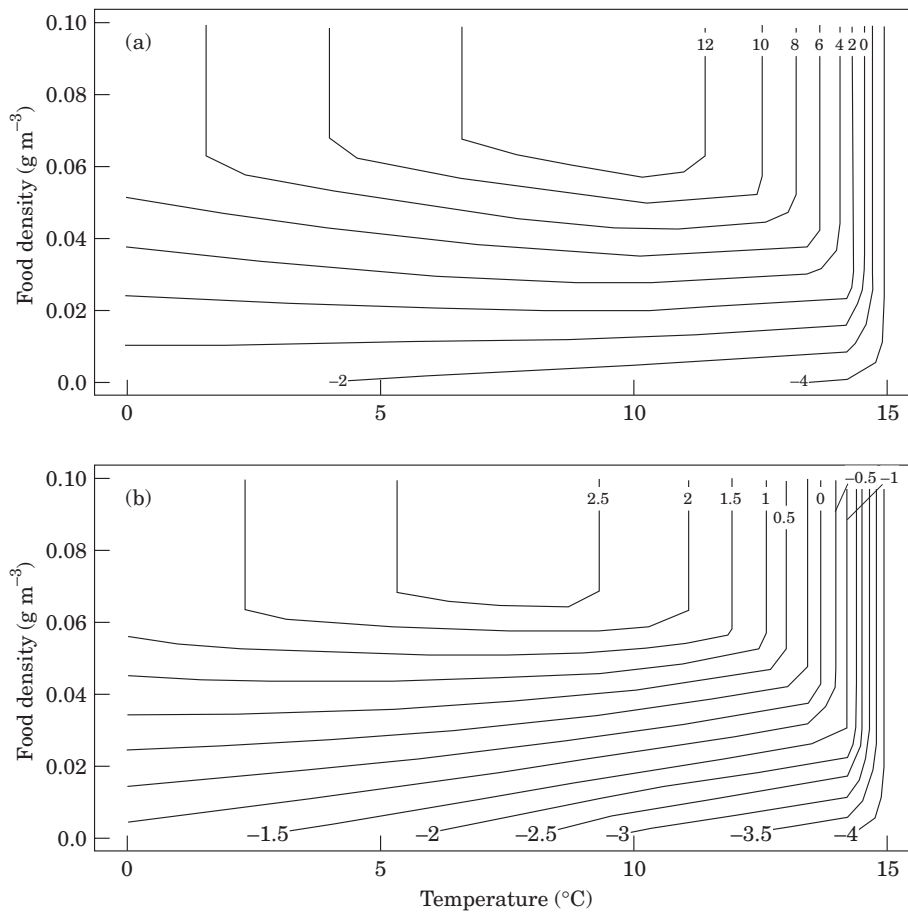


FIGURE 3. Simulated age-0 pollock growth (% body wt d^{-1}) as a function of temperature ($^{\circ}C$) and food density ($g\ m^{-3}$). Results are shown for a 1 g (a) and for a 5 g (b) age-0 pollock.

25.0% (at unlimited food density) of body weight per day for a 1 g age-0 pollock, while it ranged from 0 to 8.4% of body weight per day for a 5 g age-0 pollock in absent and unlimited food density, respectively. As imposed in the model setting, fish swimming speed was a function of both temperature and body size, if the water temperature was colder than $10\ ^{\circ}C$, while it was a function of only fish body size, if the water temperature was greater than $10\ ^{\circ}C$. Thus, maximum fish swimming speed depended on fish body size only, and it ranged from 5.2 to $8.7\ cm\ s^{-1}$ for a 1 and 5 g fish, respectively. Active metabolic rate was a function of activity multiplier, which in turn was positively related to swimming speed (Equation 4). Consequently, maximum activity was a function of fish body size only, if $T > r_{tl}$. Predicted maximum activity factor varied from 1.7 to 2.4 for a 1 g and for a 5 g fish, respectively.

The total respiration sub-model presented in Equation 4, was tested against water temperature and fish body size, by measuring the percent of total fish

ingestion (I) invested for total respiration under non-maximal food density ($0.06\ g\ m^{-3}$). These percentages ranged from 21.8 at $0\ ^{\circ}C$ to 97.7 at $14\ ^{\circ}C$. The higher percentages were reached by larger fish (5 g) at the highest temperature. Smaller fish (1 g) had overall lower percentages, ranging from 21.8% at $0\ ^{\circ}C$ to 41.3% at $14\ ^{\circ}C$, due to lower activity multiplier and to higher consumption rate.

Age-0 pollock predicted growth rate ranged from -4.4% to 13.1% of body weight per day in 1 g fish, while it ranged from -4.2% to 2.7% of body weight per day in 5 g fish (Figure 3). Growth saturation was reached at a prey density of about $0.06\ g\ m^{-3}$ for both small and large juveniles. Temperature at which growth was highest was considerably lower in smaller fish than in larger ones, $9.5\ ^{\circ}C$ in 1 g fish as opposed to $7.9\ ^{\circ}C$ in 5 g fish.

Model implementation and validation

Estimates of age-0 pollock growth potential, based on the average zooplankton configuration, showed a

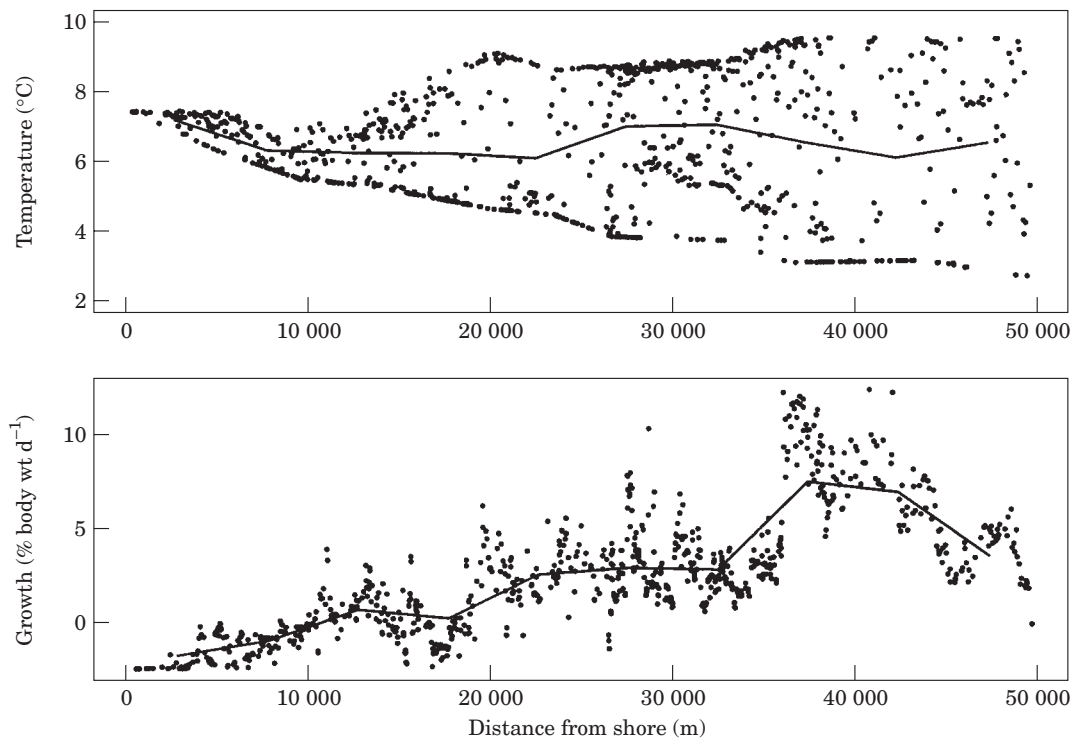


FIGURE 4. Upper panel: ambient temperature of all age-0 pollock shoals detected along Line A, September 1995. Lower panel: estimated daily growth potential of all age-0 pollock shoals along the same line and time of the year. In both panels, each dot indicates average value beneath a single fish school. Solid line indicates running average on a 2500 m distance bin.

considerable effect of spatial variability on model output. Hydroacoustic surveys indicated that fish were more abundant in the inshore and front habitats while zooplankton were more abundant in the offshore habitat (Figure 2). Consequently, age-0 pollock growth potential was from two to four times higher for fish residing in the offshore region than for those residing in the inshore and frontal regions of the sampled transect (Figure 4). Throughout the transect, average fish school temperature was rather constant and ranged between 6.12 and 7.17 °C. However the temperatures of schools residing in the offshore habitat had higher variation due to the sharp thermocline present in the area (Figure 4). Growth of fish schools residing in the offshore region also had the highest variation, most likely because of the sharp thermal gradient present in the area.

The pattern of age-0 pollock predicted growth along Line A was independently repeated in age-0 pollock growth indices. In particular, pollock in the offshore habitat had significantly higher age-specific length than in both the inshore ($P=0.024$) and the front ($P<0.0001$) habitats, while pollock collected at the front had significantly smaller age-specific length than in the inshore habitat ($P=0.011$) (Figure 5).

With respect to Fulton index, pollock in the offshore habitat also had higher indices than in the inshore habitat ($P=0.014$), but there were no differences between the front and the offshore ($P=0.875$) habitats (Figure 5).

Prey density was the environmental variable that most affected the predicted variation in age-0 pollock growth throughout Line A. This was shown by the high recovery of spatial variation in a model scenario run at homogeneous temperature and age-0 pollock size, but variable prey density (Figure 6). In contrast, fish size, and in particular water temperature had lower contribution in recovering spatial variation of age-0 pollock growth (Figure 6).

Spatial resolution analysis

The spatial pattern of predicted age-0 pollock growth potential along the transect was sensitive to the different spatial resolutions implemented in the model (Figure 7). In particular, about 2/3 of the spatial variation in growth potential, measured as the SAR between the highest (60 000 cells) and the lowest (1 cell) implemented spatial resolution, was quickly recovered going from the 1 cell to 500 cell scenarios.

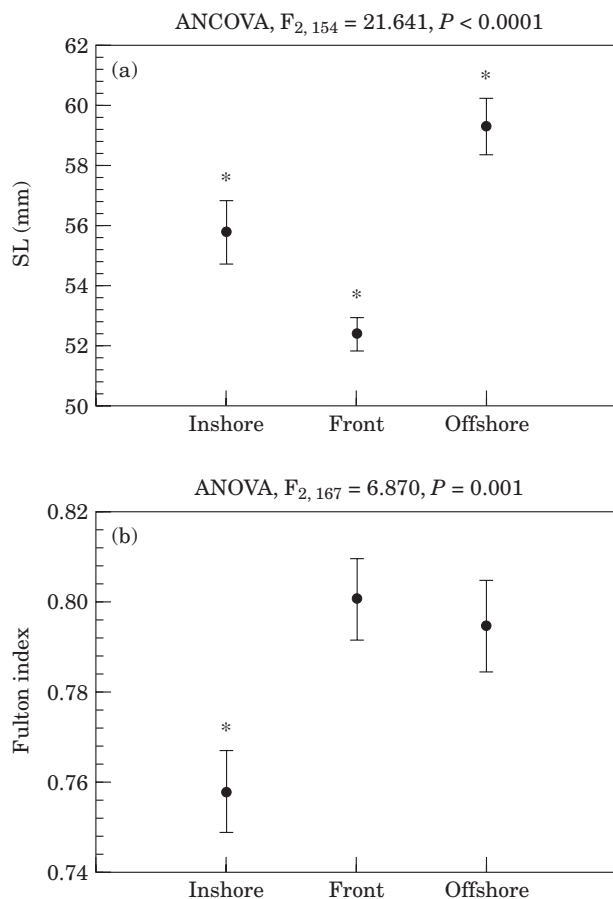


FIGURE 5. Least square adjusted mean of age-specific standard length (SL) (a) and Fulton condition index (b), from age-0 pollock collected at three hydrographic locations along Line A. Within a panel, significant differences among mean comparisons are indicated with an asterisk (Tukey, $\alpha=0.05$).

However, beyond the 500 cell scenario (cell size: 1000 m \times 8 m), the gain in spatial variation progressed at a considerably slower rate (Figure 8).

Discussion

Corroboration of forage and bioenergetics model

Predicted age-0 pollock food consumption corroborates well with independent field and laboratory estimates of age-0 pollock consumption. Ciannelli *et al.* (1998) calculated that food consumption of age-0 pollock in the Gulf of Alaska varied between 16% to 6% of body weight per day for fish growing from 0.95 to 4.29 g during one month. These feeding rates proved to be 2/3 of the predicted age-0 pollock maximum consumption rate predicted in the Gulf of Alaska model. Although the Gulf of Alaska study and

this work were built on a similar bioenergetics model, estimates of fish food consumption were derived from entirely different principles. In the Gulf of Alaska consumption was calculated to fit observed growth, while in this study fish consumption was derived from a forage model, thus while being independently assessed the two estimates are comparable. Brodeur *et al.* (2000) also estimated age-0 pollock food consumption based on gut evacuation rates, from fish collected during 3 years of sampling around the Pribilof Islands. Their estimates of age-0 pollock daily consumption for a 1 g fish ranged from 1.4 to 2.5% of body weight per day. However, these estimates can be too low, probably because of the inaccuracy in weighing small amounts of stomach contents found in the fish stomachs. In this area, growth rates of a 1 g age-0 pollock may be on the order of 4–5% body weight per day (Miriam Doyle, pers. comm., NOAA AFSC, 7600 Sand Point Way NE, Seattle WA 98115). Thus the previous estimates of age-0 pollock food consumption, based on gut evacuation time, would not be sufficient to sustain the observed fish growth rate.

Model output showed that metabolic rate of age-0 pollock, expressed as a percentage of total ingestion, increased exponentially above 10 °C, especially for larger fish. This modelling result agrees with the notion that large age-0 pollock are less adapted to warmer water than small age-0 pollock, since the respiration to consumption ratio in larger fish is rather unsustainable at high water column temperatures. In the field, smaller juvenile pollock tend to reside in the upper water column, while larger juvenile pollock either reside in deeper and colder water or perform diel vertical migrations (Brodeur & Wilson, 1996, 1999; Schabetsberger *et al.*, 2000). Also, model output indicated that the maximum growth temperature was considerably lower in larger fish than it was in smaller ones, 9.5 °C in 1 g fish as opposed to 7.9 °C in 5 g fish. These results still validate the notion that larger juvenile pollock become progressively better adapted to lower temperature, probably in preparation for winter season.

Important processes have been omitted from the model mainly due to lack of experimental information. For example, the bioenergetic model can be further improved if more information on age-0 pollock swimming speed versus water column temperature is included. Also, the effects of environmental variability on predator reactive distance (r) and on prey capture probability (P), have not been modelled. Reactive distance of fish can change according to water turbidity (Utne-Palm, 1999; Sweka & Hartman, 2001), light intensity (Utne, 1997), fish size (Breck & Gitter, 1982; Flore *et al.*, 2000) and prey type (Walton *et al.*,

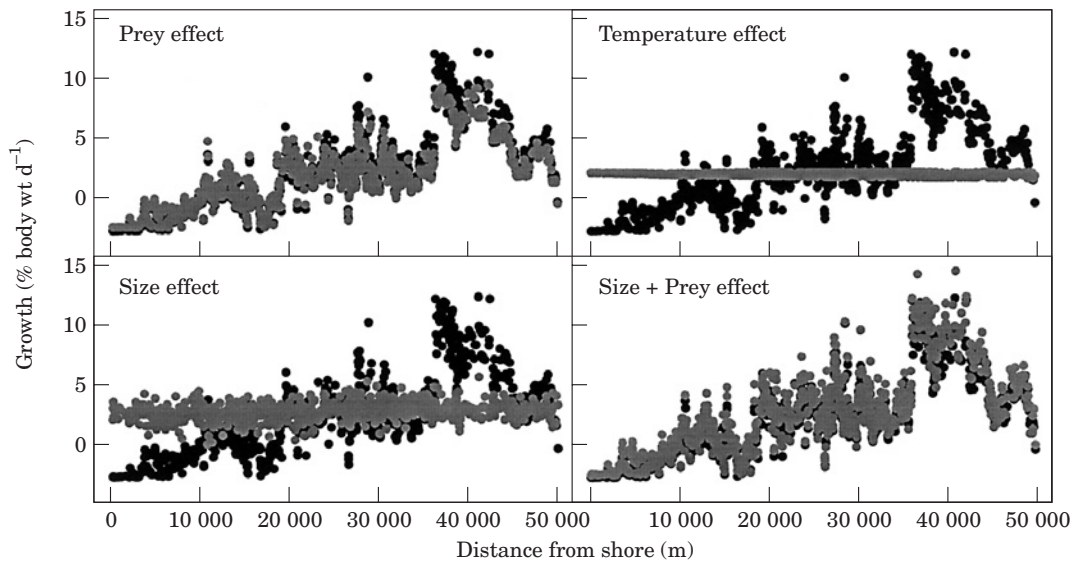


FIGURE 6. Estimated daily growth rate of age-0 pollock shoals along Line A for different environmental scenarios. Each dot indicates average growth potential beneath a single fish school. In all panels, black dots (●) indicate model results when all environmental variables are included in the model at maximum spatial resolution (full model). Grey dots (⊙) indicate model results when only the variables specified in the panel are included at the maximum spatial resolution, while the unspecified variables are homogeneous throughout the transect (partial model).

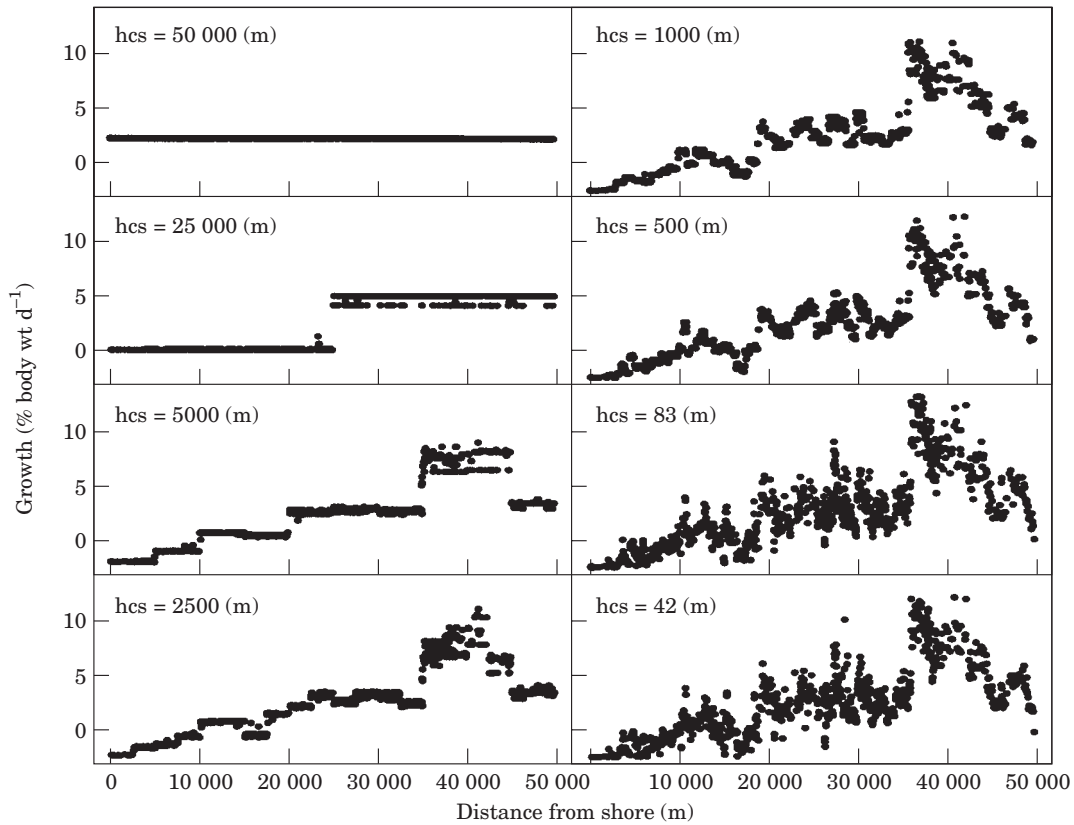


FIGURE 7. Estimated age-0 pollock growth potential along Line A, at various spatial resolutions indicated as horizontal cell size (hcs) on each panel. Each dot indicates average growth potential below a single fish school.

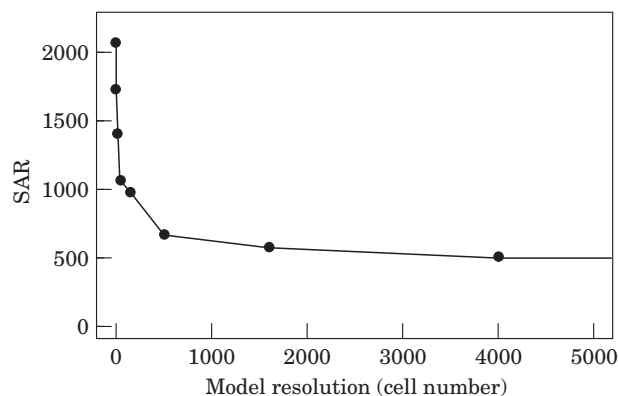


FIGURE 8. Sum of Absolute Residuals (SAR) between estimates of age-0 pollock growth potential at the maximum implemented spatial resolution (60 000 cells) and the resolution specified on the x-axis. To gain better clarity at the lower end of the spatial resolution (low cell number), the x-axis upper limit (5000 cells) is set to be lower than the maximum resolution investigated (60 000 cells).

1997) in a fashion which has already been modelled for several other species (Aksnes & Utne, 1997; Fiksen *et al.*, 1998; Fiksen & Folkvord, 1999). However, to date there are no experimental studies done on pollock to look at dependence of r to environmental variables. Given the high sensitivity of consumption estimates to changes in r (square power in Equation 2) it becomes of high priority defining such processes in juvenile pollock.

Model implementation

Results of the model implementations to the Pribilof Islands scenario indicated that in 1995, habitat diversity had the potential to drastically affect age-0 pollock growth. On average, fish residing in the offshore region of Line A could experience a four-fold increase in growth potential compared to fish residing farther inshore. Modelling output of age-0 pollock growth potential were corroborated from results of other independent growth indicators collected in same area and during same time. These indexes also showed a significant habitat effect, with offshore juvenile pollock experiencing higher than average length-specific weight and age-specific length (Figure 5). The agreement of model predictions with other independent indicators of age-0 pollock growth, besides validating the model, also indicated that age-0 pollock were residing long enough in a specific portion of Line A, so that their growth was modified according to the habitat energetics.

Several assumptions were adopted to generate the model prediction. Firstly, it was assumed that age-0's

from the inshore and offshore regions had equally time and feeding exposure to zooplankton. In reality, fish residing inshore could have longer overlap (and probably longer feeding time) with zooplankton because in this region juvenile pollock had access to the entire water column, while offshore juveniles were confined mainly above the thermocline and overlapped only during nighttime with zooplankton (Swartzman *et al.*, 1999b). Nevertheless, age-0's were residing at high density in the inshore region of Line A and could have depleted the co-occurring zooplankton biomass within few days of foraging (Ciannelli, pers. obs.). Therefore, a longer exposure time between fish and zooplankton at the inshore region could increase density-dependent limitation for food, and ultimately curtail growth of age-0 pollock.

Another important assumption of the model was the use of an arbitrary calibration factor (z) to convert zooplankton from backscatter units into biomass units. Based on the value of zooplankton density, and ultimately on the value of z , some non-linearities between fish growth and food density could arise. For example, if offshore food density were higher than the feeding threshold, there would be a saturating response of fish growth (Figure 3) and the difference between the inshore and offshore estimated age-0 pollock growth could be drastically reduced. To validate model predictions against the calibration factor I performed a model run using a wide range of z and equal age-0 size throughout the transect (to avoid a size effect on growth predictions). Results showed that age-0 pollock growth remained substantially higher offshore as long as z was contained within 0.1 to five times the value originally used (Figure 9). At the lowest extreme of 0.1 times the original calibration factor there would not be enough zooplankton in the water to sustain pollock growth. Such a scenario was considered unrealistic. At the highest extreme of five times the original calibration factor, average zooplankton biomass throughout the transect would be 0.13 g m^{-3} , a number within the range of possible values for age-0 pollock prey around the Pribilof Islands (Schabetsberger *et al.*, 2000). Consequently, it is possible that the high difference in age-0 pollock potential growth between the inshore and offshore portion of Line A was an artifact of the model calibration. However, such possibility should be unlikely because it would contrast the empirical evidence of fish growth and condition indices (Figure 5). Furthermore, as mentioned above, at the time the survey took place, it was estimated that age-0 pollock were already depleting their food supply at the inshore portion of the transect while they had plentiful food offshore.

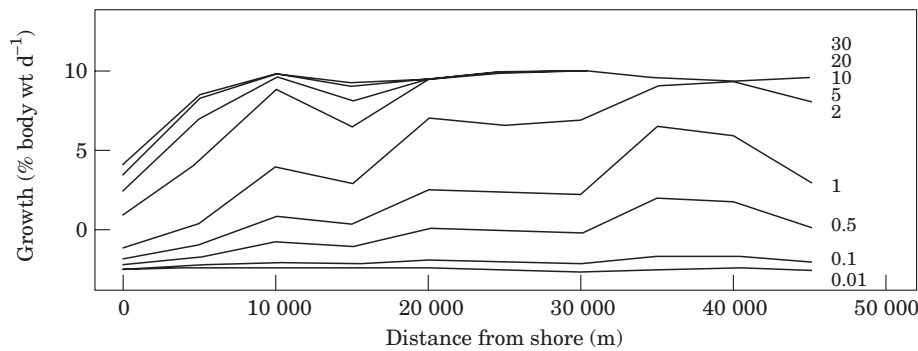


FIGURE 9. Results of model simulations showing the effects of zooplankton calibration (z), expressed as a factor of the original value used, on average distribution of age-0 pollock growth potential along Line A.

Size-selective mortality is thought to affect survival of early life stages of fish and ultimately recruitment dynamics into the adult stage (Houde, 1987). Hence, it is reasonable to assume that juvenile fishes tend to distribute in space so to optimize their growth and thereby increase their fitness (Brandt, 1993). However, I found that age-0 pollock were following a distribution that was opposite to the one that would enhance their growth. Evidently, other factors had to be considered to explain the distribution of age-0 pollock along the studied transect. It is not uncommon for fish to occupy habitats at sub-optimal growth conditions, often motivated by high predation, physical transport or competitions with other species (for a review see Sogard, 1994). It is possible that any of these factors could have contributed in shaping the distribution of juvenile pollock along Line A. For example, there are several groundfish species, such as adult walleye pollock and arrowtooth flounder (*Atheresthes stomias*), that reside in high numbers around the Pribilof Islands and that actively feed on juvenile pollock (Lang *et al.*, 2000). Also, physical transport due to tidal motion can be strong north of the Islands (Kowalik & Stabeno, 1999). And finally, the waters around the Pribilof Islands are rich in potential planktivorous competitors of age-0 pollock, such as small and large jellyfish or chaetognaths (Brodeur *et al.*, 1999; Schabetsberger *et al.*, 2000).

Spatial resolution analysis

Averaging across space can result in disruptions of predicted growth variability along a spatial gradient: the lower the model input resolution, the lower the spatial variability of model output. Thus, for this application, the question at issue was to what extent the estimated pattern in age-0 pollock growth variability along Line A was sensitive to changes in the modelled spatial resolution (i.e. cell size)? The SAR

analysis indicated that model results were highly sensitive to changes in cell size, but only at the larger range of cell size (low cell number). In contrast, an increase in model resolution beyond the 2500–1000 horizontal cell size (160–500 cell number) did not result in rapid gain of spatial variation, as shown by the abrupt change in slope of the SAR versus model resolution function (Figure 8). I suggest that this change of slope occurring at the 2500–1000 horizontal cell size, was representative of a spatial scale at which important physical and biological boundaries were crossed. The extent of these boundaries depended on both the nature of the process involved and the temporal scale over which the process was monitored. In this study, sampling took place over two weeks and most of the observed variation of age-0 pollock growth was due to prey density. Thus, it is proposed that over the time span of two weeks, sufficient spatial variation of prey density to determine changes in age-0 pollock growth, occurred beyond about 2500 m horizontal distance bins. However, the extent of spatial thresholds should change with year and season, according to the spatial heterogeneity of the modelled environment. In general, low environmental variability should result in larger spatial thresholds (Mason & Brandt, 1996).

Overall this study has met the objective of developing a spatially-explicit bioenergetics model to quantify the effect of habitat heterogeneity on estimates of age-0 pollock growth. The spatial sensitivity analysis led to the quantification of spatial thresholds beyond which model predictions became biased. The identification of such thresholds has practical and theoretical applicability. Practical, because it produces insight on how finite the sampling design should be in order to get unbiased predictions of fish growth potential (Brandt, 1993). Theoretical, because it leads to new questions aimed to understand what generates the threshold in the first place. Possible mechanisms

around the Pribilof Islands could be hydrography along the transect or zooplankton patchiness. The model developed in this study proved to be effective in reproducing and simulating age-0 pollock growth scenarios around the Pribilof Islands. Applying the model to other years and locations of the Pribilof Islands would generate new research questions and hypotheses to better understand the effect of growth on age-0 pollock distribution around the islands. Even though prey density and fish potential growth did not seem to control age-0 pollock distribution in 1995 north of St. Paul, it could still be possible that in other years or locations, habitat energetics become an important factor. However, such analysis requires a field data set more extensive than the one used in this study, with multiple years and contrasting hydrography.

Acknowledgements

I am grateful to Gordon Swartzman for the use of the hydroacoustic data and to Miriam Doyle for the use of age-length data. I thank the technical and scientific crew of the NOAA Research vessel *Miller Freeman*, and in particular Matt Wilson and Richard Brodeur, who directed the sampling. I am grateful to Anne Christine Utne-Palm for providing information on fish reactive distance and to Dan Schindler and Matt Wilson for comments on the spatial resolution analysis. Earlier drafts of this manuscript were improved through helpful comments of Richard Brodeur, Gordon Swartzman, Janet Duffy-Anderson, Art Kendall and two anonymous reviewers. This research was sponsored by NOAA's Coastal Ocean Program and is contribution FOCI-B408 to Fisheries-Oceanography Coordinated Investigations.

References

- Aksnes, D. L. & Utne, A. C. W. 1997 A revised model of visual range in fish. *Sarsia* **82**, 137–147.
- Boisclair, D. 2001 Fish habitat modeling: from conceptual framework to functional tools. *Canadian Journal of Fisheries and Aquatic Sciences* **58**, 1–9.
- Brandt, S. B. 1993 The effect of thermal fronts on fish growth: a bioenergetics evaluation of food and temperature. *Estuaries* **16**, 142–159.
- Brandt, S. B. & Mason, D. M. 1994 Landscape approaches for assessing spatial patterns in fish foraging and growth. In *Theory and Application of Fish Feeding Ecology*. Number 18 (The Belle W. Baruch Library in Marine Sciences, eds), pp. 103–131.
- Brandt, S. B., Mason, D. M. & Patrick, V. E. 1992 Spatially-explicit models of fish growth rate. *Fisheries* **17**, 23–33.
- Breck, E. J. & Gitter, M. J. 1982 Effects of fish size on the reactive distance of bluegill (*Lepomis macrochirus*) sunfish. *Canadian Journal of Fisheries and Aquatic Sciences* **40**, 162–167.
- Brodeur, R. D. & Wilson, M. T. 1996 A review of the distribution, ecology and population dynamics of age-0 walleye pollock in the Gulf of Alaska. *Fisheries Oceanography* **5** (Supplement 1), 148–166.
- Brodeur, R. D. & Wilson, M. T. 1999 Pre-recruit walleye pollock in the Eastern Bering Sea and Gulf of Alaska Ecosystems. Proceedings of GLOBEC International Marine Science Symposium on Ecosystem Dynamics, pp. 238–251.
- Brodeur, R. D., Wilson, M. T., Napp, J. M., Stabeno, P. J. & Salo, S. 1997 Distribution of juvenile pollock relative to frontal structure near the Pribilof Islands, Bering Sea. In *Proceedings of the International Symposium on the Role of Forage Fishes in Marine Ecosystems*. Alaska Sea Grant Pub. AK-SG-97-01, pp. 573–589.
- Brodeur, R. D., Mills, C. E., Overland, J. E., Walters, G. E. & Schumacher, J. D. 1999 Evidence of a substantial increase in gelatinous zooplankton in the Bering Sea, with possible links to climate change. *Fisheries Oceanography* **8**, 296–306.
- Brodeur, R. D., Wilson, M. T. & Ciannelli, L. 2000 Spatial and temporal variability in feeding and condition of age-0 walleye pollock (*Theragra chalcogramma*) in frontal regions of the Bering Sea. *ICES Journal of Marine Science* **57**, 256–264.
- Brodeur, R. D., Wilson, M. T., Ciannelli, L., Doyle, M. & Napp, J. M. In press. Interannual and regional variability in distribution and ecology of juvenile pollock and their prey in frontal systems of the Bering Sea. *Deep Sea Research II: Topological Studies in Oceanography*.
- Ciannelli, L., Brodeur, R. D. & Buckley, T. W. 1998 Development and application of a bioenergetics model for juvenile walleye pollock. *Journal of Fish Biology* **52**, 879–898.
- Coyle, K. O. & Cooney, R. T. 1993 Water column scattering and hydrography around the Pribilof Islands, Bering Sea. *Continental Shelf Research* **13**, 803–827.
- Davis, N., Myers, K. W. & Ishida, Y. 1998 Caloric value of high-seas salmon prey organisms and simulated salmon ocean growth and prey consumption. *North Pacific Anadromous Fish Commission Bulletin* **1**, 146–162.
- Decker, M. B. & Hunt, G. L. Jr. 1996 Foraging by murrelets (*Uria* spp.) at tidal fronts surrounding the Pribilof Islands, Alaska, USA. *Marine Ecology Progress Series* **139**, 1–10.
- Fiksen, Ø. & Folkvord, A. 1999 Modelling growth and ingestion processes in herring *Clupea harengus* larvae. *Marine Ecology Progress Series* **184**, 273–289.
- Fiksen, Ø., Utne, A. C. W., Aksnes, D. L., Eiane, K., Helvik, J. V. & Sundby, S. 1998 Modelling the influence of light, turbulence and ontogeny on ingestion rates in larval cod and herring. *Fisheries Oceanography* **7**, 355–363.
- Flint, M. V., Sukhanova, I. N., Kopylov, A. I., Poyarkov, S. G., Whitley, T. E. & Napp, J. M. In press. Plankton mesoscale distributions and dynamics related to frontal regions in the Pribilof ecosystem, Bering Sea. *Deep Sea Research II: Topical Studies in Oceanography*.
- Flore, L., Reckendorfer, W. & Keckeis, H. 2000 Reaction field, capture field, and search volume of 0+ nase (*Chondrostoma nasus*): effects of body size and water velocity. *Canadian Journal of Fisheries and Aquatic Sciences* **57**, 342–350.
- Gerristen, J. & Strickler, R. 1976 Encounter probability and community structure in zooplankton: a mathematical model. *Journal of Fisheries Research Board Canada* **34**, 73–82.
- Gieske, J., Huse, G. & Fiksen, Ø. 1998 Modelling spatial dynamics of fish. *Reviews in Fish Biology and Fisheries* **8**, 57–91.
- Hewett, S. W. & Johnson, B. L. 1992 Fish Bioenergetics Model 2, an upgrade of a generalized bioenergetics model of fish growth for microcomputers. University of Wisconsin Sea Grant Technical Report Number WIS-SG-92-250, 79 pp.
- Houde, E. D. 1987 Fish early life dynamics and recruitment variability. *American Fisheries Society Symposium* **2**, 17–29.
- Houde, E. D. 1989 Subtleties and episodes in the early life of fishes. *Journal of Fish Biology* **35** (Supplement A), 29–38.
- Kowalik, Z. & Stabeno, P. 1999 Trapped motion around the Pribilof Islands in the Bering Sea. *Journal of Geophysical Research* **C11**, 25667–25684.
- Lang, G. M., Brodeur, R. D., Napp, J. M. & Schabetsberger, R. 2000 Variation in groundfish predation on juvenile walleye pollock relative to hydrographic structure near the Pribilof Islands, Alaska. *ICES Journal of Marine Science* **57**, 265–271.

- Mason, D. M. & Brandt, S. B. 1996 Effects of spatial scale and foraging efficiency on the predictions made by spatially-explicit models of fish growth rate potential. *Environmental Biology of Fish* **45**, 283–298.
- Mason, D. M., Goyke, A. & Brandt, S. B. 1995 A spatially explicit bioenergetics measure of habitat quality for adult salmonines: comparison between Lake Michigan and Lake Ontario. *Canadian Journal of Fisheries and Aquatic Sciences* **52**, 1572–1583.
- McLaughlin, R. L., Grant, J. W. A. & Noakes, D. L. G. 2000 Living with failure: the prey capture success of young brook charr in streams. *Ecology of Freshwater Fish* **9**, 81–89.
- Ney, J. J. 1993 Bioenergetics modeling today: Growing pains on the cutting edge. *Transaction of the American Fisheries Society* **122**, 736–748.
- Ryer, C. H. & Olla, B. L. 1997 Altered search speed and growth: social versus independent foraging in two pelagic juvenile fishes. *Marine Ecology Progress Series* **153**, 273–281.
- Ryer, C. H. & Olla, B. L. 1998 Effect of light on juvenile walleye pollock shoaling and their interaction with predators. *Marine Ecology Progress Series* **167**, 215–226.
- Schabetsberger, R., Brodeur, R. D., Ciannelli, L., Napp, J. M. & Swartzman, G. L. 2000 Diel vertical migration and interaction of zooplankton and juvenile walleye pollock (*Theragra chalcogramma*) at a frontal region near Pribilof Islands, Bering Sea. *ICES Journal of Marine Science* **57**, 1283–1295.
- Sinclair, E., Loughlin, T. & Percy, W. 1993 Prey selection by northern fur seals (*Callorhinus ursinus*) in the eastern Bering Sea. *Fishery Bulletin* **92**, 144–156.
- Sogard, M. 1994 Use of suboptimal foraging habitats by fishes: consequences to growth and survival. In *Theory and Application of Fish Feeding Ecology*. Number 18 (The Belle W. Baruch Library in Marine Sciences, eds), pp. 103–131.
- Stabeno, P. J., Schumacher, J. D., Salo, S. A., Hunt, G. L. & Flint, M. 1999 The physical environment around the Pribilof Islands. In *The Bering Sea: Physical, Chemical and Biological Dynamics* (Loughlin, T. R. & Ohtani, K., eds). Alaska Sea Grant Press. AK-SG-99-03. pp. 193–216.
- Swartzman, G. L., Brodeur, R. D., Napp, J. M., Walsh, D., Hewitt, R., Demer, D., Hunt, G. & Logerwell, E. 1999a Relating predator and prey spatial distributions in the Bering Sea using acoustic backscatter data. *Canadian Journal of Fisheries and Aquatic Science* **56** (Supplement 1), 188–198.
- Swartzman, G. L., Brodeur, R. D., Napp, J. M., Hunt, G., Demer, D. & Hewitt, R. 1999b Spatial proximity of age-0 walleye pollock (*Theragra chalcogramma*) to zooplankton near the Pribilof Islands, Bering Sea, Alaska. *ICES Journal of Marine Science* **56**, 545–560.
- Sweka, J. A. & Hartman, K. J. 2001 Influence of turbidity on brook trout reactive distance and foraging success. *Transaction of the American Fisheries Society* **130**, 138–146.
- Traynor, J. T. & Smith, D. 1996 Summer distribution and relative abundance of age-0 walleye pollock in the Bering Sea. In *Ecology of Juvenile Walleye Pollock* (Brodeur, R. D., Livingston, P. A., Loughlin, T. R. & Hollowed, A. B., eds). *NOAA Technical Report* **126**, 57–59.
- Utne, A. C. W. 1997 The effect of turbidity and illumination on the reaction distance and search time of the marine planktivore *Gobiusculus flavescens*. *Journal of Fish Biology* **50**, 926–938.
- Utne-Palm, A. C. 1999 The effect of prey mobility, prey contrast, turbidity and spectral composition on the reaction distance of *Gobiusculus flavescens* to its planktonic prey. *Journal of Fish Biology* **54**, 1244–1258.
- Viitasalo, M., Kiørbe, T., Flinkman, J., Pedersen, L. W. & Visser, A. W. 1998 Predation vulnerability of planktonic copepods: consequences of predator foraging strategies and prey sensory abilities. *Marine Ecology Progress Series* **175**, 129–142.
- Yamazaki, H. & Squires, K. D. 1996 Comparison of oceanic turbulence and copepod swimming. *Marine Ecology Progress Series* **144**, 299–301.
- Walton, E. W., Emiley, J. A. & Hairston, N. G. Jr. 1997 Effect of prey size on the estimation of behavioral visual resolution of bluegill (*Lepomis macrochirus*). *Canadian Journal of Fisheries and Aquatic Sciences* **54**, 2502–2508.
- Ware, D. M. 1975 Growth, metabolism, and optimal swimming speed of pelagic fish. *Journal of the Fisheries Research Board of Canada* **32**, 33–41.
- Winberg, G. G. 1956 *Rate of Metabolism and Food Requirements of Fishes*. Belorussian University, Minsk, 253 pp. (Translated by Fisheries Research Board of Canada, Translation. No. 164, (1960).